Simultaneous determination of human erythrocyte deformability and adhesion energy: a novel approach using a microfluidic chamber and the "glass effect"

Carolina M. Londero[1,2,3] · Bibiana D. Riquelme*[1,2]

[1] Área Física, Facultad de Cs Bioquímicas y Farmacéuticas (UNR) – Rosario, Argentina. Suipacha 531. 20000 - Rosario, Santa Fe, Argentina.

2 Instituto de Física Rosario (CONICET, UNR) – Rosario, Argentina. Bv. 27 de febrero 210 bis. 20000 - Rosario, Santa Fe, Argentina

[3] Facultad de Cs Exactas, Ingeniería y Agrimensura (UNR) – Rosario, Argentina. Pellegrini 250. 20000 - Rosario, Santa Fe, Argentina.

* Corresponding author: briquel@fbioyf.unr.edu.ar, riquelme@ifir-conicet.gov.ar

Abstract

The simultaneous determination of adhesion and deformability parameters of erythrocytes was carried out through a microfluidic device which uses an inverted optical microscope with new image acquisition and analysis technologies. Also, an update of the models describing erythrocyte adhesion and deformation was proposed. Measurements were carried out with red blood cells suspended in saline solution with human serum albumin at different concentrations. Erythrocytes adhered to a glass surface were subjected to different low shear stress (from 0.04 to 0.25 Pa), causing cellular deformation and dissociation. The maximum value obtained of the Erythrocyte Deformability Index was 0.3, and that of the adhesion energy per unit area was 1.1×10^{-6} Pa.m, both according to previous works. The obtained images of RBCs adhered to glass reveal that the adhesion is stronger in a single point of the cell, suggesting a ligand migration that concentrates the adhesion in a '*spike-like tip*' in the cell. Moreover, adhesion energy results indicate that the energy required to separate erythrocytes in media with a lower albumin concentration is greater. Both results could be explained by the mobility of membrane receptors.

Keywords: microfluidic chamber, red blood cell deformation, red blood cell adhesion, hemorheology

Introduction

The erythrocyte (red blood cell, RBC) is a non-nucleated human cell whose structure and function has been characterized in detail and described by several biological-physical models [1-4]. Many studies in this exciting field continue to produce new insights into the RBC features, both in health and disease. Furthermore, because of its simplicity, research on RBCs could shed new light into the function of the membrane in other cell types by providing important information about other complex problems [1].

All blood cells interact among themselves and with the epithelial cells by mechanisms that depend on adhesion molecules as well as on the several forces involved in the interaction, such as Van der Waals attraction forces and repulsive electrostatic forces [5-7]. In physiological conditions, erythrocytes at stasis state aggregate by facing their concave surfaces in structures similar to stacks of coins called *rouleaux* [8]. Moreover, it has been shown that the viscoelastic characteristics of the erythrocyte provide it with high deformability under low shear stress, dissipating internal energy without changing its surface-area-to-volume ratio [9-11]. Nevertheless, these properties could be altered by changes in the structural proteins of the RBC. For this reason, in several diseases, it is worth knowing to what extent the erythrocyte deformability and adhesion capability have been involved.

Several methods have been developed for measuring either aggregation or deformation of erythrocytes based on different physical properties [12-16]. However, the results obtained for RBC deformability with diverse techniques can be difficult to compare due to different sample manipulation, type/magnitude of stresses applied and influence of various factors (shape, internal medium, and membrane) on deformation [17]. Furthermore, in the case of red blood cell adhesion, no "standard" suspension has been developed that allows direct comparison of determinations using different techniques. Therefore, there is a great interest in the development of a device that allows the determination of both erythrocyte parameters,

deformability and adhesion, simultaneously [18,19]. This could lead to establishing standardized processes that provide valuable information on hematological and vascular diseases.

Consequently, the aim of this work was to simultaneously determine erythrocyte deformability and adhesion parameters using a microfluidic chamber. Furthermore, the method proposed here is based on a modified theoretical model and on the phenomenon of RBC adhesion to glass without crenation (RBCs appear with a rounder form and spiny projections on the cell surface) by "glass effect" [20].

Theoretical model

Several models have been described to quantify the deformability of RBCs. Among them, the Evans and Hochmuth model [2] is useful to describe the RBC viscoelastic behavior in the physiological range at low shear stresses.

The erythrocyte membrane maintains its osmotic balance in physiological conditions, therefore restricting the RBC volume variation. Furthermore, the erythrocyte lipid bilayer has great resistance to change its surface area per molecule. Consequently, these restrictions define RBC surface-area-to-volume ratio and limit the smallest diameter the cell can acquire when deformed [9]. It has been shown that at shear stresses under 3 Pa in isotonic conditions, variations in the RBC surface-area-to-volume ratio has no impact on its deformability [10]. Under these conditions, RBCs deform with no change in these parameters, providing the appropriate conditions for the study of its shape variation. Based on this fact, Skalak *et al*. in 1973 and Evans in 1975 demonstrated that, in the plane of the membrane, the human erythrocyte behaves like an isotropic material [21,22]. In this simplified conception, the membrane cannot change the lipid bilayer thickness, modifying only the shape of a surface element. They modeled the projected erythrocyte as a circle when it is in stasis ($L \cong l$) and as an ellipse when it is under shear stress ($L' > l'$) as defined in Figure 1a. Also, they proposed a

deformability ratio λ that relates the dimensions of the deformed ellipse to its original shape. If the shape is a circle with diameter D, then $D = L = l$ and the major and minor axes of the ellipse can be written as a function of λ through $L'=D\ \lambda$ and $l'=D\ /\lambda$. From this, the erythrocyte deformability index (*EDI*) can be defined as:

$$EDI = \frac{L'-l'}{L'+l'} = \frac{D\ \lambda-\frac{D}{\lambda}}{D\ \lambda+\frac{D}{\lambda}} = \frac{\lambda^2-1}{\lambda^2+1} \tag{1}$$

In this model, the RBC viscoelastic behavior is described under low shear stresses and physiological conditions by the internal tension, T, as a function of three parameters: λ, μ_m (the membrane elastic modulus) and η_m (the surface viscosity) through the following expression:

$$T = \mu_m(\lambda^2 - \lambda^{-2}) - 4\,\eta_m \frac{d(\ln \lambda\,)}{dt} \tag{2}$$

Under stationary deformation regime, the equation can be reduced to a simple function of the *EDI*:

$$T = \mu_m(\lambda^2 - \lambda^{-2}) = \mu_m \frac{4\ EDI}{1-EDI^2} \tag{3}$$

If we assume the internal tension to be uniformly distributed along the erythrocyte transversal area of perimeter p and outer surface S, then a linear relation can be established between T and the applied stress σ given by:

$$\sigma\ \frac{S}{2} = T\ p \Rightarrow \sigma = K_{RBC}\ \frac{EDI}{1-EDI^2} \tag{4}$$

where K_{RBC} is a newly defined constant named “RBC shape constant”.

In this work, the *EDI* was considered as a function of σ to perform a second-order Taylor approximation. From the resulting quadratic equation, the following simple relation was obtained for low values of shear stress:

$$EDI \cong \frac{\sigma}{K_{GR}} \tag{5}$$

Another important property of RBCs is adhesion, which allows them to interact with the vessels and blood cells. However, this adhesion property of erythrocytes is found to be altered in different pathologies, as stated before, even modifying the morphology of erythrocyte aggregates. This behavior can be explained based on the classical theory of fracture and Williams's study on adhesion of two elastic bodies [23]. Macroscopically, Skalak's model [8,24,25] describes the process appropriately since it includes all the energy variations in the calculation of the work required to separate adhered erythrocytes suspended in a physiological fluid (plasma, saline solution, etc.). In the particular case of conservative external forces, the differential equation that relates the adhesion energy per unit area (γ) to the stored elastic energy (U), and the contact area between cells (A_C) is:

$$0 = \frac{dU}{dt} - \gamma \frac{dA_c}{dt} \tag{6}$$

When studying the separation of an erythrocyte from glass (under a laminar flow that generates a shear stress σ), the adhesion process has already happened. Therefore, the work done to separate the cell by the action of σ (noted as W_σ) can be related to U, transforming Eq. 6 in the following equation:

$$\gamma = \frac{\partial W_\sigma}{\partial A_c}\Big|_{T,\mu} \approx \frac{\langle W_\sigma \rangle}{A_0} = \frac{F\frac{\delta}{2}}{A_0} = \frac{\sigma\, A_d\, \delta}{2\, A_0} \tag{7}$$

where a mean value approximation was made, and A_0 is the initial area of the adhered cell. W_σ is given by the force $F=\sigma A_d$, where A_d is the area of the deformed cell (Figure 1b). A linear relation was also considered between F and the cell displacement (δ) for separation of around 50% [5,26].

Materials and Methods

Biological Samples

Five blood samples obtained by venous puncture from healthy donors (20-30 years old, non-smokers, non-drinkers and unmedicated) were used. These samples were anticoagulated with EDTA and after 5 minutes of centrifugation at 500 g, plasma and red blood cells were separated for later use. Sample selection, collection, and handling were carried out in agreement with the recommendations of the *International Expert Panel for Standardization of Hemorheological Methods* [17]. This study had the approval of the Ethics Committee of the Faculty de Biochemical and Pharmaceutical Sciences of the National University of Rosario (Res. Nº 422/2017) and all donors signed the corresponding "Informed Consent" for their participation.

RBC suspensions

Erythrocytes need a special resuspension medium that allows both deformability and adhesion energy measurements [27] to avoid RBCs morphological alteration in the absence of plasma proteins (echinocyte formation due to *glass effect* [20,28,29]). Based on previous reports [14,30], the selected suspension media consisted of saline solution (0.90% w/v of NaCl, 308 mOsm/L or 9.0 g per liter, with pH 7.4 and 308 mOsm/L, produced by *Laboratorios Roux-Ocefa S.A*) with human serum albumin (purified and distributed by *Laboratorio de Hemoderivados UNC*). Three suspension media were used corresponding to albumin concentrations of 0.05, 0.10 and 0.20 % v/v.

Microfluidic chamber

The microfluidic chamber was designed based on the chamber proposed by Hochmuth *et al.* [31] and used in several studies [14, 26, 30]. This device, described in detail in the bibliography, has an interior cavity of h = (0.25 ± 0.01) mm height, a = (18.00 ± 0.05) mm width and (45.00 ± 0.05) mm length, with a glass slide as a base. The glass surface consisted of a borosilicate glass slide used for microscopy (standard slides 76 x 45 mm, *neoLab*, Germany), without any additional treatment, and is attached to the device using a vacuum

pump and a sealing membrane (PTFE sheet, *Direct Plastics Ltd*, England) [14,30]. Inside the microfluidic chamber, RBCs adhere to the glass surface, and cellular dissociation is a direct consequence of the shear stress parallel to the glass base produced by an infusion pump (*780100C Digital Single Syringe Infusion Pump*), allowing the progressive detachment of the cell as it deforms [32]. The shear stress is defined in a laminar regime and is calculated considering the thickness and width of the channel, the flow rate Q and the viscosity η of the suspension medium from the following equation deduced by Sung *et al.* [26]:

$$\sigma = \frac{6\,Q\,\eta}{h^2\,a} \tag{8}$$

The cell suspensions were prepared suspending 8 µL of RBCs in 20 µL of saline solution with human serum albumin at 0.2, 0.1 and 0.05% v/v. Each suspension was placed in a syringe of the infusion pump and the channel of the chamber was carefully filled in order to avoid bubble formation. The flow chamber was placed with the glass slide down in an inverted optical microscope (*Union Optical* - Japan, 40x objective) with a camera (*Mikoba 300 CMOS 3.0*) connected to a computer. To guarantee RBC adhesion to the glass surface of the channel, a waiting time of 15 minutes was established before starting the flow. Digital images were captured using the *IS Capture 3.0* software.

Image acquisition and Measurements

The image acquisition software was designed to capture a series of 10 images every 5 seconds (resolution of 2048x1536) in a preselected visual field, where an image of the cells at stasis state (i.e. without σ) was previously obtained. The infusion pump was then started, and after 10 seconds the software began the acquisition. Once the series was finished, the value of the flow rate was modified and the image acquisition process repeated for shear stresses calculated between 0.04 Pa and 0.25 Pa.

Previously, the viscosities of media with albumin at 0.05, 0.10 and 0.20 % were measured (at 115.2 s^{-1} in a rotational viscometer Brookfield DV-II), obtaining 0.83, 0.82 and 0.88 mPa.s

respectively, with 0.01 mPa.s of uncertainty. The corresponding σ were calculated and no significant variations were observed between the three different media. Consequently, mean values of σ were used in the following determinations.

In the flow chamber, the cell progressively lengthens in the direction of the flow as σ increases, taking the shape of a prolate spheroid, producing an ellipse in the observation plane of the microscope. Thus, the shape of the deformed RBC can be described by a single parameter, EDI (Eq. 1), determined by the measurements depicted in Figure 1a.

In the microfluidic chamber, the shear stress applied is parallel to the interface of the cell and the glass. Then, when σ is higher, the difference between the length of the ellipse axes is larger, and, therefore, the EDI is higher. The images of deformed RBC under σ were overlapped to those obtained at stasis state (i.e. without deformation, $\sigma = 0$), as sketched in Figure 1b. Then, the area of the ellipse projected by the cell at stasis state (A_0) and deformed state (A_d), and the displacement length (δ) were digitally measured (FIJI, ImageJ2) to calculate γ from Eq. 7. Each area was measured by overlapping an ellipse on the cell image with the corresponding software tool (FIJI, ImageJ2).

Data processing and Statistical analysis

A mean value of the EDI was calculated for seven cells from the same sample suspended in equal media and subjected to the same shear stress. These results were expressed as Mean ± SD and represented vs. σ for each suspension used. Each plot was fitted with a linear regression because of the linearity of the model introduced in Eq. 5. Likewise, mean values of γ were plotted as a function of σ and linear fits were overlapped for a better analysis of the data.

Results and Discussion

Erythrocyte Deformability

Figure 2 presents an example of the images obtained for a cell in different states of deformation inside the microfluidic chamber, showing a schematic description for determination of the axes lengths (L and l in stasis state, L' and l' when deformed) used to calculate the *EDI*. The images in Figure 2 show that the adhesion is stronger in a single point of the cell, suggesting a ligand migration in the cell membrane that concentrates the adhesion at this point, as previously theorized by DiMilla *et al.* [32]. Specifically, the bonds on the cell membrane would move on the surface accumulating in a small area, producing a '*spike-like tip*' in the cell.

The mean values of the *EDI* as a function of the σ obtained for all samples are presented in Figure 3 for RBCs suspended in saline-albumin solutions at 0.05, 0.1 and 0.2 % v/v. This graph shows that the erythrocyte deformability index increases with an increase in shear stress, regardless of the amount of albumin present in the suspension. For cells at stasis state, the length of both axes is the same, yielding an *EDI* value close to 0. The maximum value of the *EDI* obtained is about 0.3 at a shear stress of (0.164 ± 0.4) Pa for RBCs suspended in saline-albumin solution at 0.1% v/v. Plots presented in Figure 3 correspond to the average results of the calculated parameter for different cells at different stages of life in the samples. Then, a non-monotonic plot is obtained, and the linear regressions provide a generalized behavior of a population of RBCs in a sample. Also, the result of the essay with the solution at 0.1% of albumin shows an initial flat region, which would indicate the presence of yield stress. This behavior is characteristic of a Bingham body and thus of the cytoplasm, as observed by Rubinson and Baker [33]. Nonetheless, individual cell studies can be carried out successfully with the technique here presented.

The updated Evans-Hochmuth model deduced here (Eq. 5) proves to be valid only for certain regions of each plot, due to a change in slope between samples and a nonzero intercept. This could be explained by the fact that the model considers RBCs with cylindrical symmetry,

which does not usually occur in the analyzed cells, even less when they have adhered to the flat surface of the glass. Furthermore, the mechanical properties of the erythrocytes would be caused by the tubulin connected to the outer membrane that would causes the Bingham body behavior [34].

Erythrocyte Adhesion Energy

Figure 4 presents an example of the image of a deformed RBC overlapped with the image of the same RBC in stasis state. Also, this figure shows a schematic description of the measurements performed to obtain γ (the area of the cell at stasis state (A_0), at the deformed state (A_d), and the displacement length (δ)).

The mean values of γ as a function of σ are presented in Figure 5 for each suspension medium used. These plots show that the adhesion energy increases linearly with the shear stress applied during the separation process. This result suggests that the RBC membrane deforms, adjusting their shape to have a constant value of $\frac{A_d\,\delta}{2\,A_0}$, which is the slope of the graph according to Equation 7. This significant result, together with the observed '*spike-like tip*' phenomenon, could be explained considering the mobility of the RBC membrane receptors, according to what was proposed by Sackmann *et al*. [35]. The mean values of the slope obtained from the linear fittings of *EDI* and γ plots for each saline-albumin solution are shown in Table 1 (expressed as Mean ± SD) [17,27]. The intercept values, obtained from the plot γ vs σ, were practically equal to zero according to Figure 5, where the linear fittings pass through the origin. An important aspect from the results in Table 1 is the different effect of the albumin concentration on the measured parameters: for *EDI*, the mean value of the slope increases, but decreases for γ. Results from γ show that the average slope value decreases from (2.5 ± 0.8) μm to (1.3 ± 0.6) μm when the albumin concentration increases, but this decrease is not significant (p-value = 0.0885) due to the high uncertainty in the determinations. Nevertheless, this tendency could indicate that the energy required to separate

erythrocytes in media with a lower albumin concentration is greater. This result is consistent with the fact that the presence of plasmatic proteins in the medium decreases the adhesion phenomenon, reducing the *glass effect* [27]. Besides, the previously suggested ligand migration could be affected by the concentration of proteins in the suspension medium; however, the chemical mechanism responsible for this effect cannot be corroborated with the current data.

Moreover, the values of γ obtained in this work (from 0.2 10^{-7} Pa.m to 3.7 10^{-7} Pa.m at 0.1 % v/v albumin concentration) are in the same range as those measured for RBC adhesion to a layer of hyaluronate (over the glass slide) by D'Arrigo *et at.* [14], whose results range from 0.09 to 2.71 10^{-7} Pa.m.

Conclusions

In the present work, the values of two parameters representing deformability (*EDI*) and adhesion energy (γ) of normal human red blood cells were simultaneously obtained using a novel technique that involves a microfluidic chamber and the "glass effect".

This microfluidic chamber provides more complete information than other methods since it allows an *in vitro* and real-time visualization of two erythrocyte processes (adhesion and deformability) under different conditions. The parameters simultaneously obtained may be of great importance for the understanding and analysis of possible alterations in RBCs due to vascular pathologies (diabetes, hypertension). Consequently, this study could help design appropriate medical treatments to prevent possible microcirculatory alterations.

The microfluidic chamber used in this work provides simultaneous information on the deformability and adhesion energy of an individual cell. Therefore, the implementation of this new technology could allow the development of specific studies of cell adhesion and dissociation from different substrates and with different ligands. Particularly, this research

could contribute to the improvement of biomedical devices (stems, catheters, prostheses) and to the development of studies of biocompatibility and functionality of new biomaterials.

Acknowledgments

The authors would like to thank Dr. Mabel D'Arrigo for performing the blood draws and Dr. Analía I. Alet and the staff from the English Department of the Facultad de Ciencias Bioquímicas y Farmacéuticas (UNR) for the language correction of the manuscript. Carolina Londero would also like to thank the "Nuevo Banco de Santa Fe" for the Technological Innovation Scholarship received to carry out a previous optimization and validation of the microfluidic chamber used in this work.

Funding: This study was funded by the National University of Rosario.

Conflict of Interest: The authors declare that they have no conflict of interest.

References

1. Mohandas, N., Gallagher, P.G. (2008) Red cell membrane: past, present, and future. *Blood* 112(10), pp. 3939–3948. doi: 10.1182/blood-2008-07-161166
2. Evans, E.A. & Skalak, R. (2018) *Mechanics and Thermodynamics of Biomembranes*, pp. 1-254. eBook ISBN 9781351074339. DOI: 10.1201/9781351074339
3. Riquelme, B.D., Valverde, J., Rasia, R.J. (1998) Complex viscoelasticity of normal and lectin treated erythrocytes using laser diffractometry. *Biorheology*, 35 (4-5), pp. 325-334. doi: 10.1016/S0006-355X(99)80014-6
4. Castellini, H.V., Riquelme, B.D. (2018) Study of non-linear viscoelastic behavior of the human red blood cell. *Quantitative Biology,* arXiv:1810.07760v1.
5. Sans-Sabrafen, J., Besses Raebel, C., Vives Corrons, J.L. (2006) *Hematología clínica.* Quinta Ed. Elsevier. ISBN 9788481747799

6. Meiselman, H., Neu, B., Rampling, M., Baskurt, O. (2007) RBC aggregation: Laboratory data and models. *Indian Journal of Experimental Biology* 45(1), pp. 9-17.

7. Lebensohn, N., Re, A., Carrera, L., Barberena, L., D´Arrigo, M., Foresto, P. (2009) Ácido siálico sérico, carga aniónica y agregación eritrocitaria en pacientes diabéticos e hipertensos. *Medicina* 69(3), pp. 331–334.

8. Skalak, R., Zarda, P.R., Jan, K.M., Chien, S. (1981) Mechanics of rouleau formation. *Biophysical Journal* 35(3), pp. 771–781. doi:10.1016/s0006-3495(81)84826-6

9. Waugh, R.E., Hochmuth, R.M. (2014) Mechanics and deformability of hematocytes. In: *Biomechanics: Principles and Practices*. CRC Press. eBook ISBN 9780429110832. doi: 10.1201/b15575

10. Renoux, C., Faivre, M., Bessaa, A., Da Costa, L., Joly, P., Gauthier, A., *et al.* (2019) Impact of surface-area-to-volume ratio, internal viscosity and membrane viscoelasticity on red blood cell deformability measured in isotonic condition. *Scientific Reports* 9(1), pp. 1–7. doi: 10.1038/s41598-019-43200-y

11. Gratzer, W.B. (1981) The red cell membrane and its cytoskeleton. *The Biochemical Journal* 198(1), pp. 1–8. doi: 10.1042/bj1980001

12. Rasia, R.J. (1995) Quantitative evaluation of erythrocyte viscoelastic properties from diffractometric data: Applications to Hereditary spherocytosis and hemoglobinopathies. *Clinical Hemorheology and Microcirculation* 15(2), pp. 177–189. doi: 10.3233/CH-1995-15205

13. Kaliviotis, E., Ivanov, I., Antonova, N., Yianneskis, M. (2010) Erythrocyte aggregation at non-steady flow conditions: A comparison of characteristics measured with electrorheology and image analysis. *Clinical Hemorheology and Microcirculation* 44(1), pp. 43–54. doi: 10.3233/CH-2009-1251

14. D'Arrigo, M., Riquelme, B.D., Valverde, J., Foresto, P. (2009) Análisis de la energía de adhesión intercambiada en la unión CD44-hialuronato. *e-Universitas UNR Journal* 1(2), pp. 305–312.
15. Toderi, M.A., Castellini, H.V, Riquelme, B.D. (2017) Descriptive parameters of the erythrocyte aggregation phenomenon using a laser transmission optical chip. *Journal of biomedical optics* 22(1), art. no. 17003. doi: 10.1117/1.JBO.22.1.017003
16. Toderi, M.A., Riquelme, B.D., Galizzi, G.E. (2020) An experimental approach to study the red blood cell dynamics in a capillary tube by biospeckle laser. O*ptics and Lasers in Engineering* 127, art. no. 105943. doi: 10.1016/j.optlaseng.2019.105943
17. Baskurt, O.K., Hardeman, M.R., Rampling, M.W., Meiselman, H.J. (2007) *Handbook of Hemorheology and Hemodynamics*. 1st ed. Amsterdam: IOS Press. eBook ISBN 9781607502630
18. Riquelme, B.D., Londero, C.M. (2018) New Optical Approach to Simultaneous Determination of Deformability and Adhesion Energy of Human Erythrocytes. *Optics InfoBase Conference Papers*, Part F123-LAOP 2018. doi: 10.1364/LAOP.2018.Th4A.39
19. Alapan, Y., Little, J.A., Gurkan, U.A. (2014) Heterogeneous red blood cell adhesion and deformability in sickle cell disease. *Scientific Reports* 4, art. no. 7173. doi: 10.1038/srep07173
20. Eriksson, L.E. (1990) On the shape of human red blood cells interacting with flat artificial surfaces - the "glass effect". *Biochimica et Biophysica Acta* 1036(3), pp. 193–201. doi: 10.1016/0304-4165(90)90034-t
21. Skalak, R. (1973) Modelling the mechanical behavior of red blood cells. *Biorheology* 10(2), pp. 229–238. doi: 10.3233/BIR-1973-10215

22. Evans, E.A. (2018) Mechanics of cell deformation and cell-surface adhesion. In: P*hysical Basis of Cell-Cell Adhesion*, pp. 91-124. CRC Press. eBook ISBN 9781351075572. doi: 10.1201/9781351075572

23. Bennett, S.J., Devries, K.L. & Williams, M.L. (1974) Adhesive fracture mechanics. *International Journal of Fracture* 10, 33–43. doi: 10.1007/BF00955077

24. Skalak, R., Chien, S. (1983) Theoretical models of rouleau formation and disaggregation. *Annals of the New York Academy of Sciences* 416 (1), pp. 138-148. doi: 10.1111/j.1749-6632.1983.tb35184.x

25. Skalak, R., Zhu, C. (1990) Rheological aspects of Red Blood Cell aggregation. *Biorheology* 27(3–4), pp. 309–325. doi: 10.3233/BIR-1990-273-409

26. Sung, L.A., Kabat, E.A., Chien, S. (1985) Interaction energies in lectin-induced erythrocyte aggregation. *Journal of Cell Biology* 101(2), pp. 652–659. doi: 10.1083/jcb.101.2.652

27. Londero, C.M., D'Arrigo, M., Riquelme, B.D. (2016) Optimización del medio de suspensión para la observación de glóbulos rojos humanos frescos con microscopios ópticos. *Acta Microscópica* 25(3), pp. 151–156.

28. Ponder, E.H. (1971) *Hemolysis and related phenomena*. Second Ed. Grune & Stratton. ISBN 9780808906728

29. Wong, P. (2005) A hypothesis of the disc-sphere transformation of the erythrocytes between glass surfaces and of related observations. *Journal of Theoretical Biology* 233(1), pp. 127–135. doi: 10.1016/j.jtbi.2004.09.013

30. Danieli, V., D'Arrigo, M., Riquelme, B.D., (2009) Deformability of adhered cells study by means of digital microscopic images. *Acta Microscópica*, 18(3), pp. 261–268.

31. Hochmuth, R.M., Mohandas, N., Blackshear Jr., P.L. (1973) Measurement of the elastic modulus for red cell membrane, using a fluid mechanical technique. *Biophysical Journal* 13, pp. 747–762. doi: 10.1016/S0006-3495(73)86021-7

32. DiMilla, P.A., Barbee, K., Lauffenburger, D.A. (1991) Mathematical model for the effects of adhesion and mechanics on cell migration speed. *Biophysical Journal* 60(1), pp. 15–37. doi: 10.1016/S0006-3495(91)82027-6

33. Rubinson, K. A., Baker, P. F. (1979) The Flow Properties of Axoplasm in a Defined Chemical Environment: Influence of Anions and Calcium. *Proceedings of the Royal Society B: Biological Sciences*, 205(1160), pp. 323–345. doi:10.1098/rspb.1979.0068

34. Amaiden, M.R., Monesterolo, N.E., Santander, V.S., Campetelli, A.N., Arce, C.A., Pie, J., Hope, S.I., Vatta, M.S., Casale, C.H. (2012) Involvement of membrane tubulin in erythrocyte deformability and blood pressure. *Journal of Hypertension* 30(7), pp. 1414–1422. doi: 10.1097/HJH.0b013e328353b19a

35. Sackmann, E., Smith, A.S. (2014) Physics of cell adhesion: some lessons from cell-mimetic systems. *Soft Matter* 10(11), pp. 1644–1659. doi: 10.1039/c3sm51910d

FIGURE CAPTIONS

Figure 1. (a) Representation of a red blood cell at stasis state ($\sigma=0$) and under shear stress ($\sigma' > 0$) where L and L' are the longitudinal axes, l and l' are the transversal axes. (b) Description of the measurement of the cell area at stasis state (A_0) and deformed (A_d), and the length displaced (δ).

Figure 2. Example of the determination of the major and minor axes from RBC suspended in saline-albumin solution at 0.05% v/v, images obtained in states of stasis, and deformed under a shear stress of $(50 \pm 4)\ 10^{-3}$ Pa.

Figure 3. Plots of the mean value of *EDI* vs. σ for the different saline-albumin solutions used (0.05, 0.1 and 0.2% v/v). Lines represent the linear fittings and error bars represent the standard deviations.

Figure 4. Example of the measurement of the area of the ellipse projected by RBC suspended in saline-albumin solution at 0.05% v/v, when at stasis state (A_0) and deformed state (A_d) with the length it displaced (δ), for shear stress of $(50 \pm 4)\ 10^{-3}$ Pa.

Figure 5. Plots of the mean value of γ vs. σ for the different saline-albumin solutions used (0.05, 0.1 and 0.2% v/v). Lines represent the linear fittings and error bars represent the standard deviations.

TABLE TITLE

Table 1. Mean values of the linear regression parameters calculated from the EDI vs. σ and γ vs. σ plots (Figs. 3 and 5, respectively) for RBC suspended in the different saline-albumin solutions.

Figure 1

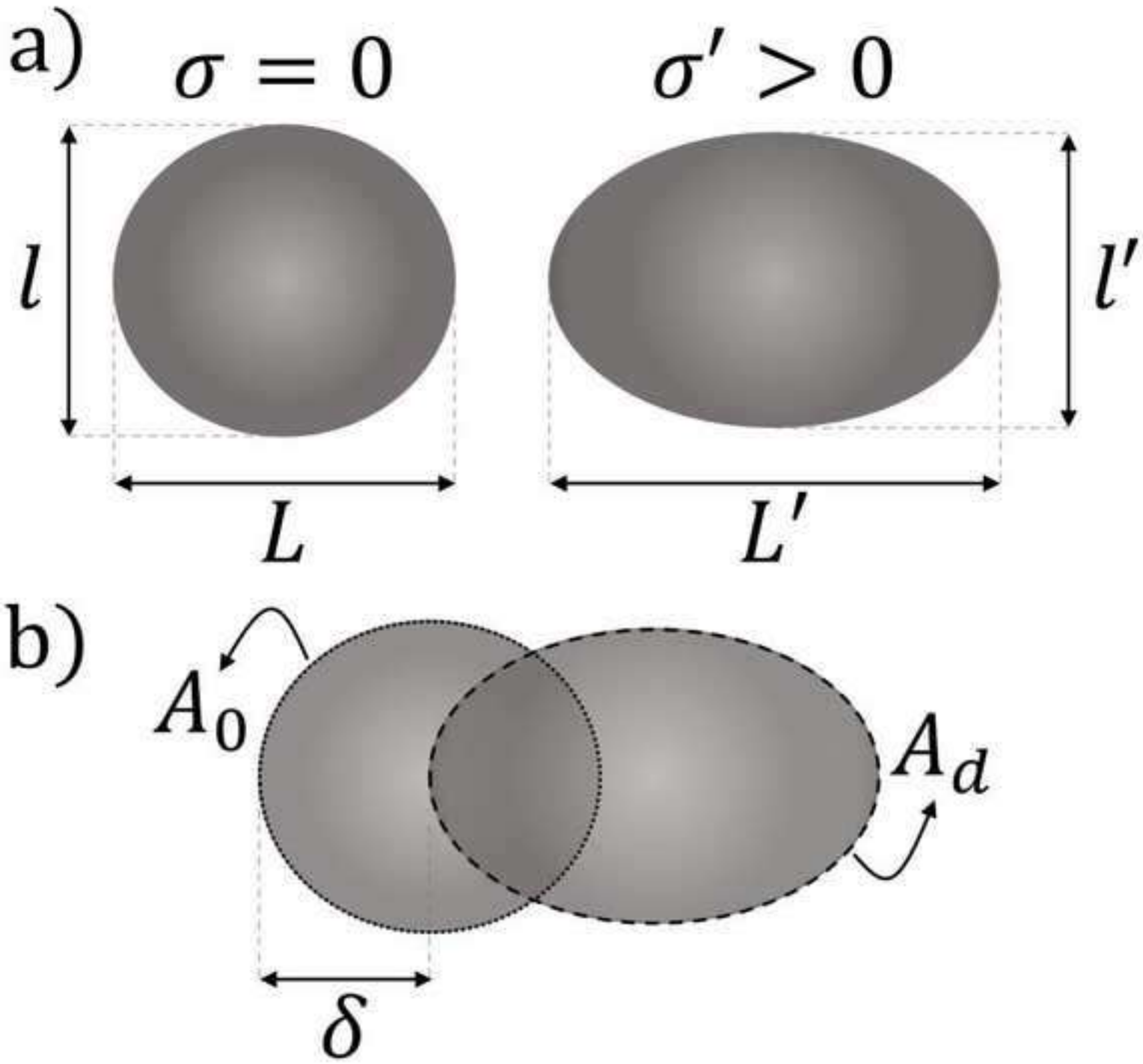

Figure 2

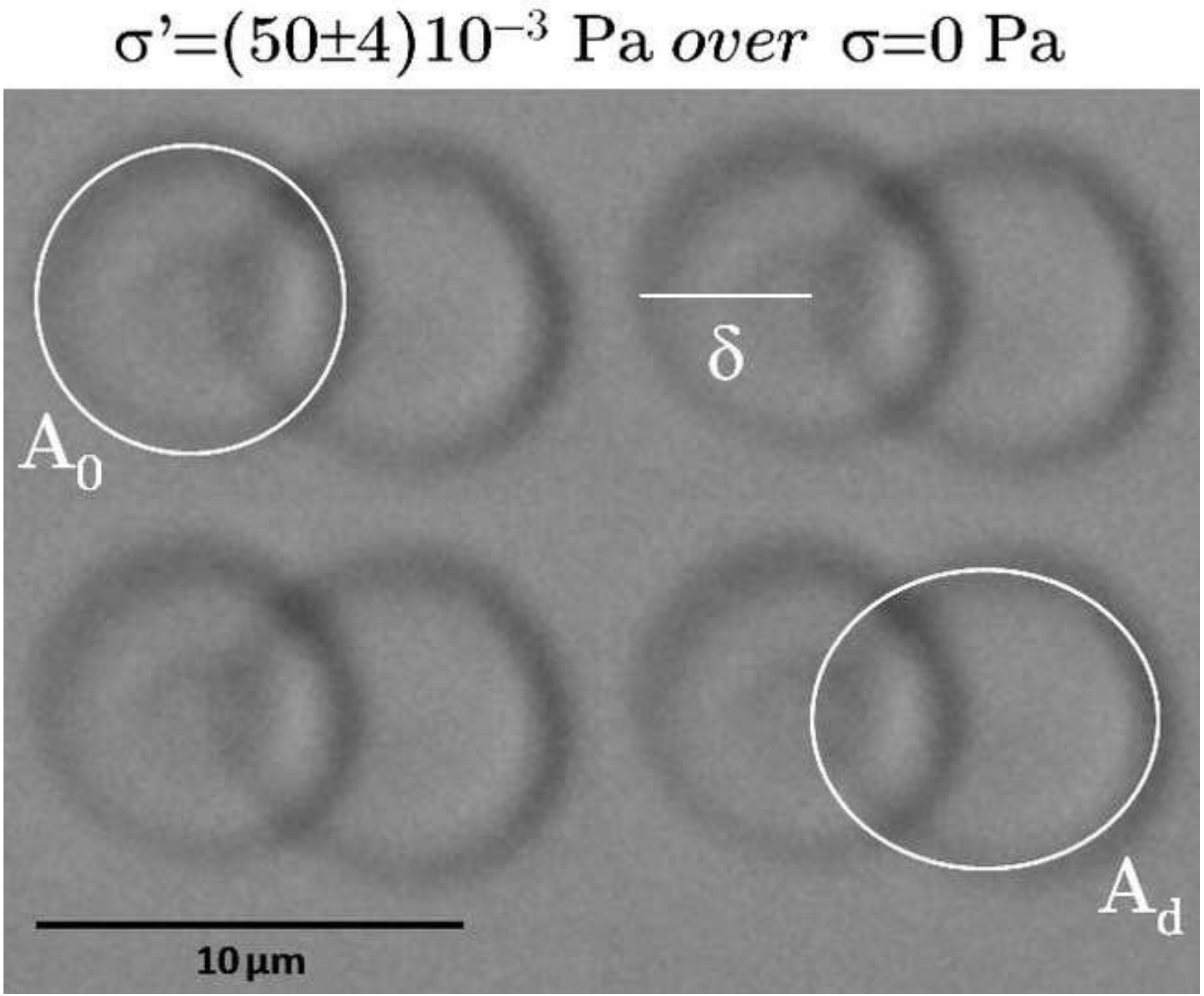

Figure 3

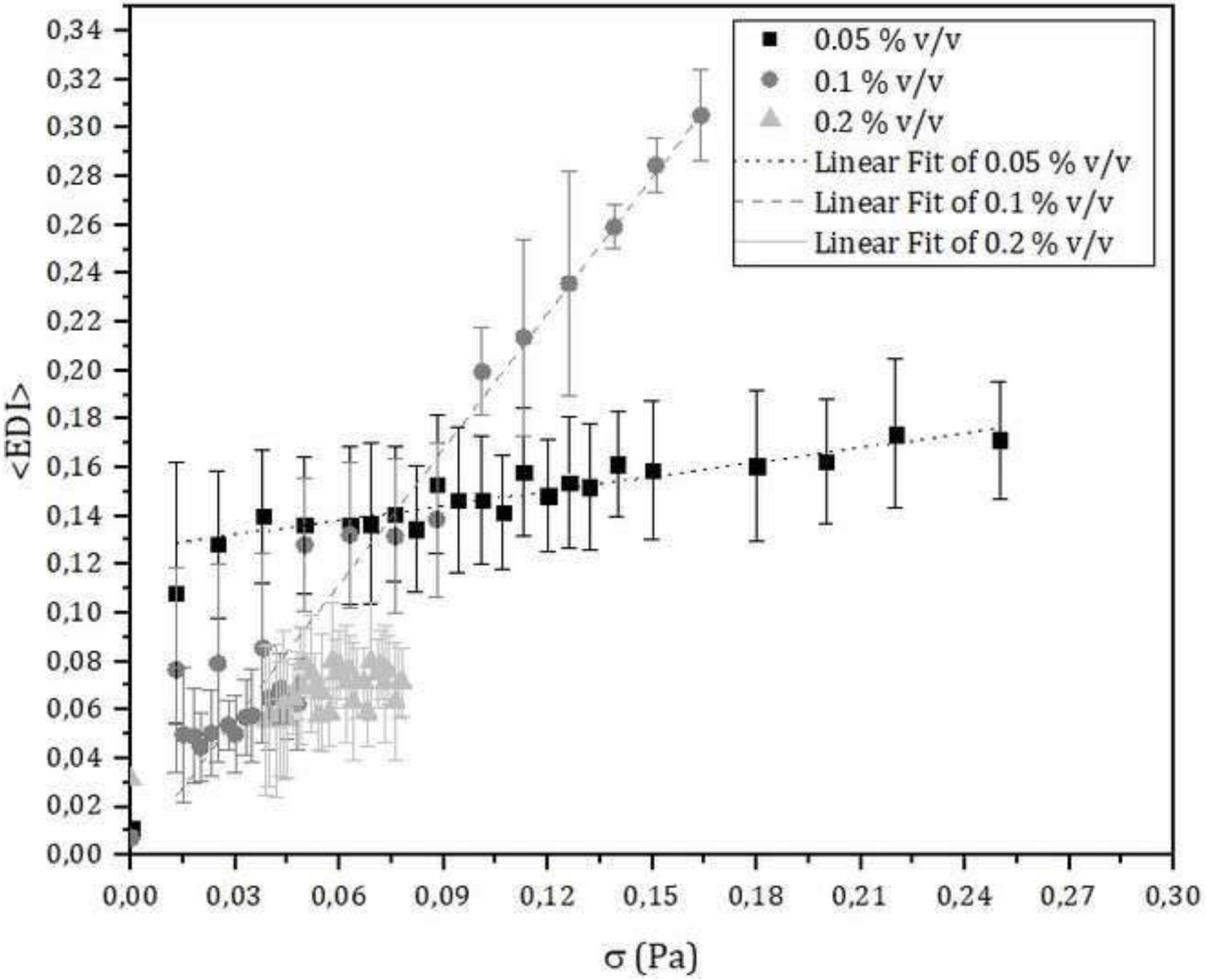
0,34
0,32
0,30
0,28
0,26
0,24
0,22
0,20
0,18
0,16
0,14
0,12
0,10
0,08
0,06
0,04
0,02
0,00
<EDI>
0,00
0,03
0,06
0,09
0,12
0,15
0,18
0,21
0,24
0,27
0,30
σ (Pa)
0.05 % v/v
0.1 % v/v
0.2 % v/v
Linear Fit of 0.05 % v/v
Linear Fit of 0.1 % v/v
Linear Fit of 0.2 % v/v

Figure 4

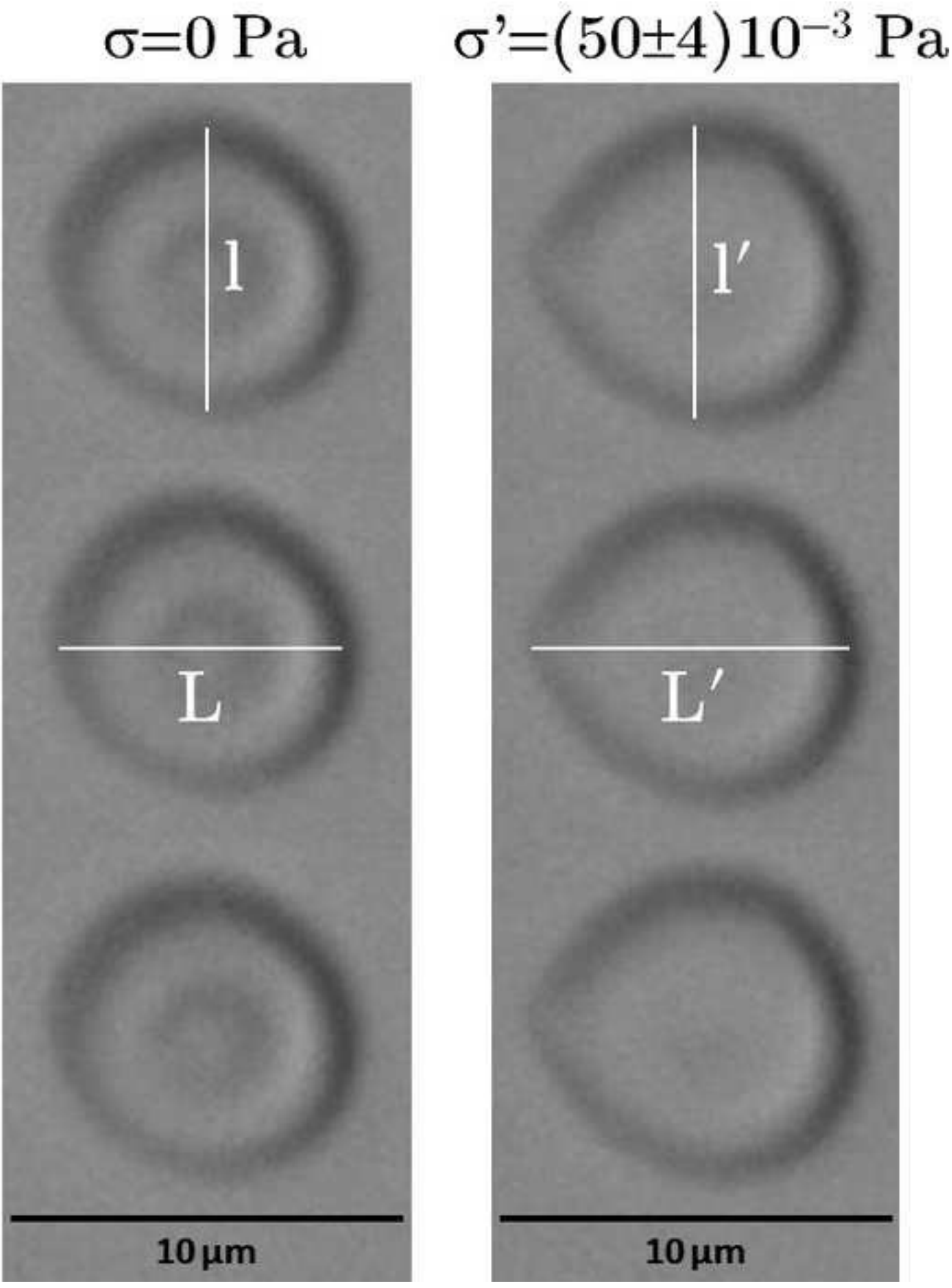

Figure 5

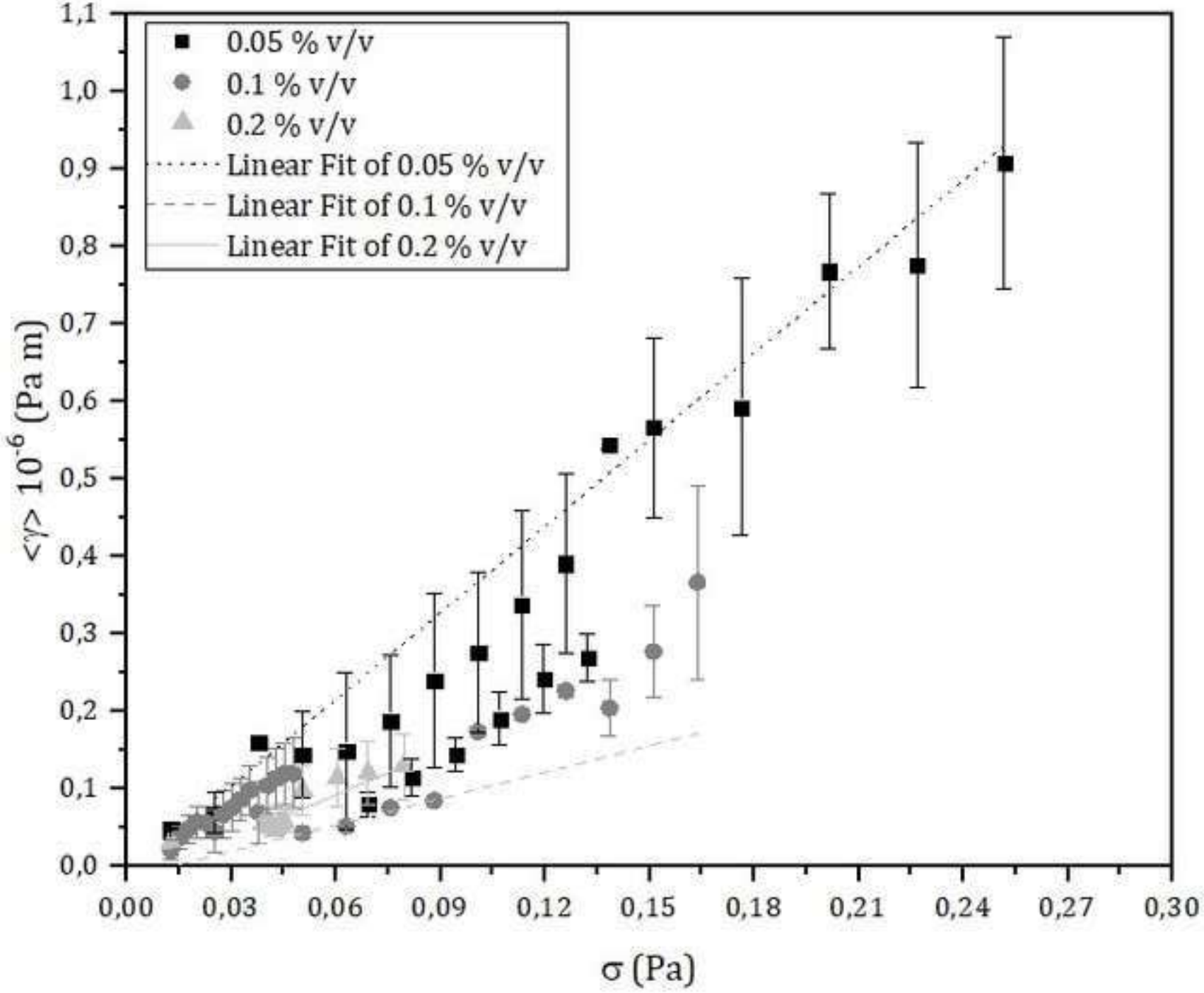
0.05 % v/v
0.1 % v/v
0.2 % v/v
Linear Fit of 0.05 % v/v
Linear Fit of 0.1 % v/v
Linear Fit of 0.2 % v/v
<γ> 10-6 (Pa m)
σ (Pa)
1,1
1,0
0,9
0,8
0,7
0,6
0,5
0,4
0,3
0,2
0,1
0,0
0,00
0,03
0,06
0,09
0,12
0,15
0,18
0,21
0,24
0,27
0,30

Table 1. Mean values of the linear regression parameters calculated from the EDI vs. σ and γ vs. σ plots (Figs. 3 and 5, respectively) for RBC suspended in the different saline-albumin solutions.

Albumin concentration % v/v	**EDI**		γ	
	Slope 1 / Pa	**Intercept**	**Slope 10^{-6} m**	**Intercept 10^{-6} Pa . m**
0.05	0.35 ± 0.09	0.115 ± 0.006	2.6 ± 0.8	-0.2 ± 0.7
0.10	1.30 ± 0.20	0.026 ± 0.009	2.0 ± 0.9	-0.4 ± 0.5
0.20	1.51 ± 0.09	0.039 ± 0.006	1.3 ± 0.6	0.9 ± 1.3